

mmWave Beam Selection in Analog Beamforming Using Personalized Federated Learning

Martin Isaksson^{*†}, Filippo Vannella^{*†}, David Sandberg^{*} and Rickard Cöster^{*}
^{*}Ericsson AB, Stockholm, Sweden

[†]KTH Royal Institute of Technology, Stockholm, Sweden
Contact: martin.isaksson@ericsson.com

Abstract—Using analog beamforming in mmWave frequency bands we can focus the energy towards a receiver to achieve high throughput. However, this requires the network to quickly find the best downlink beam configuration in the face of non-IID data. We propose a personalized Federated Learning (FL) method to address this challenge, where we learn a mapping between uplink Sub-6GHz channel estimates and the best downlink beam in heterogeneous scenarios with non-IID characteristics. We also devise FEDLION, a FL implementation of the Lion optimization algorithm. Our approach reduces the signaling overhead and provides superior performance, up to 33.6% higher accuracy than a single FL model and 6% higher than a local model.

Index Terms—beamforming, beam selection, distributed learning, federated learning

I. INTRODUCTION

The massive data traffic demands of next generation mobile networks require new technologies and deployment strategies in high-frequency bands. In particular, Millimeter Wave (mmWave) frequency bands are important for 5G mobile communication due to large available bandwidths which provide low latency, and high data rates [1]. Signals in mmWave frequency bands are affected by high path loss, and are sensitive to blockage effects in the environment. Using large antenna arrays, combined with beamforming techniques, we can focus the energy towards a receiver. This requires a beam training phase to steer the transmitter beam towards the receiver, and it is important to do this quickly with low signaling overhead.

In this paper, we investigate the problem of selecting the best mmWave downlink (DL) beam in an analog beamforming scenario, as shown in Fig. 1. Previous work often predict the best DL beam based on mmWave channel estimates, which can be difficult or costly to obtain. We leverage the correlation between different frequency bands to learn a mapping between the more easily acquired Sub-6GHz uplink (UL) channels and the mmWave DL channels, as in [2]. Using this mapping, we select the best DL beam from a pre-defined codebook. We formulate this problem as a multi-class classification problem, where the input is a channel estimate acquired from sounding reference symbols on the Sub-6GHz UL channel, and the output is a beam index used to select a column from the codebook.

Federated Learning (FL) [3], [4] has the potential to leverage decentralized datasets, such as those found in next generation mobile networks, while enhancing privacy by using client compute and storage resources. However, classical FL approaches such as Federated Averaging (FEDAVG) have

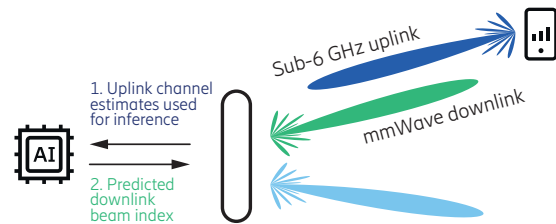


Fig. 1. Overview of the proposed mmWave beam prediction system. UL Sub-6GHz channel estimates are acquired from sounding reference symbols and used to predict the mmWave DL beam index.

limitations when data is heterogeneous and non-Independent and Identically Distributed (IID) due to the differences between clients and between groups of clients.

Personalized FL has emerged as a promising approach to address the challenges of privacy and data heterogeneity in the context of mobile networks, enabling mobile devices to collaboratively learn personalized models without compromising user privacy or transmitting raw data to a central server.

Prior work [5]–[7] solved the problem with IID data. In this paper we use the DeepMIMO [8], [9] dataset generation framework to generate a more realistic dataset where the data of each client shows non-IID characteristics.

Our hypothesis is that a single FL model cannot capture the non-IID characteristics present in this dataset. Using Iterative Federated Clustering Algorithm (IFCA) [10], we show here that we can train a set of global cluster models, and personalize this set to achieve higher performance. Furthermore, using a Mixture of Experts (MoE) [11] we can in addition to the global cluster models also utilize a purely local model as an expert.

In summary, our main contributions are as follows.

1. We adapt the problem of selecting the best mmWave analog beamforming DL beam to account for non-IID characteristics, specifically class imbalance, concept shift (same features, different label) and unbalanced data;
2. By combining a clustering technique with a MoE [11] we can adapt to non-IID characteristics in the data to achieve higher accuracy than the state-of-the-art;
3. We devise FedLion, a new FL algorithm based on EvoLved Sign Momentum (Lion) [12] as the optimization algorithm on the parameter server which achieves higher sample efficiency and accuracy than FEDAVG.

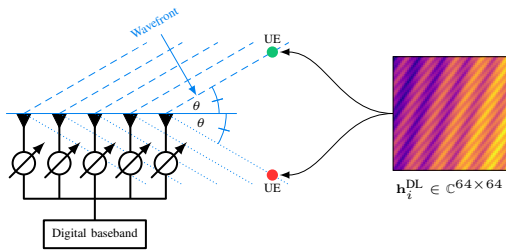


Fig. 2. **Antenna model.** Illustration of a ULA antenna and a sample of the DL channel \mathbf{h}_i^{DL} between the antenna for two UEs at the same distance from the antenna in **front of** or **behind** the antenna.

II. BACKGROUND

A. Analog beamforming and beam management

With the use of mmWave frequency bands in 5G New Radio (NR), several GHz of bandwidth becomes available. These large amounts of available spectrum means that very high peak rates and throughput can be supported. However, the effective antenna area of an antenna becomes smaller with increasing frequency for a fixed antenna gain. Hence, to maintain a given coverage the effective antenna gain has to be increased. This can be achieved by increasing the number of antenna elements and apply beamforming to the signal. Beamforming is a technique to steer the transmission (or reception) of a signal in a specific direction, see Fig. 2 for an example with a Uniform Linear Array (ULA) used in this paper. In general, this is done by adjusting the phase and amplitude of the transmitted signal at each antenna element in the antenna array. In *analog beamforming* the phase of the signal fed to each antenna element is adjusted to steer the signal in the wanted direction while the amplitude of the signal is kept constant across the antenna elements. As the number of antenna elements increases, beams tend to become narrower which increases the beamforming gain. Therefore, many narrow beams are needed for coverage, which also makes it more time-consuming to find a high-gain beam on the transmitter side.

The problem we address in this paper is how to select the optimal DL beamforming vector from a predefined codebook in order to get the best possible user experience. We use a quantized beam steering codebook [5], $\mathcal{F} = [\mathbf{f}(1), \dots, \mathbf{f}(N)]$ with $N = 64$ beamforming vectors as columns. Each element in \mathcal{F} can be written as

$$\mathcal{F}_{m,l} = \frac{1}{\sqrt{M}} e^{-i\pi m \cos \theta(l)}, \quad (1)$$

where $m \in \{0, \dots, M-1\}$ is the precoder weight index, for M transmit antennas and $\theta(l) = \frac{\pi l}{N}$ is the beam angle for beamforming vector $l \in \{0, \dots, N-1\}$.

Traditional methods. A simple and straightforward technique to find the optimal DL beam in analog beamforming is to perform an exhaustive search over the entire set of candidate beams [13]. This has large time overheads since a User Equipment (UE) will have to measure on each beam and report the strongest. Improvements include hierarchical codebooks and interactive beam-search.

Deep learning based methods. The problem of mapping channels between frequency bands was studied in for example [2] for two close frequencies. The authors of [2] also proved the existence of a channel-to-channel-mapping which was exploited in [5] to predict mmWave beams and blockages from Sub-6GHz UL channels and later in [6], where FL was used to learn the mapping and directly predict the DL beamforming vector. However, the dataset used in [5], [6] was assumed to be IID — which is not realistic. In our work, we consider a more realistic scenario with data having class imbalance and concept shift (same features, different label), and we assign each data sample to the strongest base station, see Fig. 3.

B. Problem formulation

We consider a distributed and decentralized setting with base stations as clients $k \in \{1, 2, \dots, K\}$. Each client k has access to a local data partition P_k that never leaves the client, and where $n_k = |P_k|$ is the number of local data samples.

We model the problem as a multi-class classification problem, where we have $n = \sum_{k=1}^K n_k$ input UL channel estimates $\mathbf{h}_i^{\text{UL}} \in \mathbb{C}^{64 \times 4}$, indexed by $i \in \{1, 2, \dots, n_k\}$, and output class labels y_i are in a finite set. See [8] for a detailed expression of the channel. We further divide each client partition P_k into local training and test sets and investigate the performance on the local test set in a non-IID setting.

Given the predicted beam index \hat{y}_i , we take the corresponding DL beamforming vector $\mathbf{f}(\hat{y}_i)$ and DL channel \mathbf{h}_i^{DL} (with added Additive White Gaussian Noise (AWGN)) and calculate the mean *channel capacity* for a subcarrier with bandwidth B as

$$\mathcal{R}_i(\mathbf{h}_i^{\text{DL}}, \hat{y}_i) = \frac{B}{L} \sum_{s=1}^L \log_2 \left(1 + \left| \mathbf{h}_i^{\text{DL}} [s]^\dagger \mathbf{f}(\hat{y}_i) \right|^2 \right), \quad (2)$$

where $\mathbf{h}_i^{\text{DL}} [s]^\dagger$ is the hermitian of the DL channel for the i th sample at the s th subcarrier and L is the number of subcarriers.

C. Federated Learning

The UL channel estimate can be used to estimate the position of a UE, which is a privacy concern. One way of improving privacy is to use a collaborative Machine Learning (ML) algorithm such as FEDAVG [3]. In FEDAVG, a parameter server coordinates training of a global model in a distributed, decentralized and synchronous manner over several communication rounds until convergence.

In communication round t , the parameter server selects a fraction C out of K clients as the set S_t . Each selected client $k \in S_t$ trains on n_k locally available data samples $(\mathbf{h}_i^{\text{UL}}, y_i)$, $i \in P_k$, for E epochs before an update is sent to the parameter server. The parameter server aggregates all received updates and computes the global model parameters \mathbf{w}_g . Finally, the new global model parameters are sent to all clients.

We can now define our learning objective as

$$\min_{\mathbf{w}_g \in \mathbb{R}^d} \mathcal{L}(\mathbf{w}_g) \triangleq \min_{\mathbf{w}_g \in \mathbb{R}^d} \overbrace{\sum_{k=1}^K \frac{n_k}{n} \frac{1}{n_k} \sum_{i \in P_k} \ell(\mathbf{h}_i^{\text{UL}}, y_i, \mathbf{w}_g)}^{\text{population average loss}}, \quad (3)$$

client k average loss
sample i loss

where $\ell(\mathbf{h}_i^{\text{UL}}, y_i, \mathbf{w}_g)$ is the negative log-likelihood loss function between the optimal beam index y_i , i.e., the beam achieving the highest rate, and the predicted beam index \hat{y}_i . In other words, we aim to minimize the average loss of the global model over all clients in the population.

III. METHOD

A. Federated EvoLved Sign Momentum

We devise Federated EvoLved Sign Momentum (FEDLION), a federated version of Lion [12], [14], and use this on the parameter server to replace FEDAVG. The pseudocode of FEDLION is presented in Algorithm 1, where we indicate changes needed to adapt FEDLION to work in the FL setting. We construct FEDLION in a similar way to FEDADAM, FEDYOGI and FEDADAGRAD [15] which are all federated versions of adaptive optimizers with momentum. In addition to weight decay (controlled by λ), we also decay the server-side learning rate η as training progresses. $\beta_1, \beta_2 \in [0, 1)$ are hyperparameters.

Algorithm 1 FEDLION — server

- 1: Initialize \mathbf{w}_g ▷ Initialize global model
 - 2: Initialize \mathbf{m} with zeros. ▷ Initialize momentum
 - 3: $K_s \leftarrow \lceil CK \rceil$ ▷ Number of clients to select
 - 4: **for** $t \in \{1, 2, \dots\}$ **do** ▷ Until convergence
 - 5: $S_t \subseteq \{1, 2, \dots, K\}, |S_t| = K_s$ ▷ Client selection
 - 6: **for all** $k \in S_t$ **do** ▷ For all clients, in parallel
 - 7: $\mathbf{w}_k, n_k \leftarrow k.\text{CLIENT}(\mathbf{w}_g)$ ▷ Local training
 - 8: $\Delta^k \leftarrow \mathbf{w}_k - \mathbf{w}_g$ ▷ Client update
 - 9: $n \leftarrow \sum_{k \in S_t} n_k$ ▷ Total number of samples
 - 10: $\Delta \leftarrow \frac{1}{n} \sum_{k \in S_t} n_k \Delta^k$ ▷ Update
 - 11: $\mathbf{m} \leftarrow \beta_2 \mathbf{m} + (1 - \beta_2) \Delta$ ▷ Momentum
 - 12: $\mathbf{w}_g \leftarrow \mathbf{w}_g - \eta (\text{sgn}(\beta_1 \mathbf{m} + (1 - \beta_1) \Delta) + \lambda \mathbf{w}_g)$
-

B. Personalized Federated Learning

Personalized FL offers a balance between knowledge shared among clients and models personalized to each client. Using more than one global model allows clusters of clients that are more similar within the cluster than to other clients to share knowledge that is more useful to them, and to use this as a better starting point for personalization. IFCA [10] is a clustering technique where, after the training phase, the cluster model with the lowest loss on the validation set is used for all future inferences. In IFCA, each client has access to the full set of cluster models, and the hypothesis of [7], [11] is that if a client can make use of *all* of these models we can increase

performance. However, in our beam prediction dataset, we have *concept shift* (same features, different label), a non-IID characteristic that makes the MoE select a single global cluster model expert. This implies that the conditional distribution $\mathcal{P}(y|\mathbf{h}^{\text{UL}})$ varies between clients, but $\mathcal{P}(\mathbf{h}^{\text{UL}})$ is shared [16]. Therefore, our MoE use a local model and the best global cluster model as experts, see Fig. 4b. Due to the presence of heterogeneous environments between the clients, we also expect a *concept drift* (same label, different features) non-IID characteristic, i.e. the conditional distribution $\mathcal{P}(\mathbf{h}^{\text{UL}}|y)$ varies between clients at least within the clusters, but $\mathcal{P}(y)$ is shared.

C. Models

We take the complex UL channel estimate \mathbf{h}^{UL} as input to a Convolutional Neural Network (CNN) model with architecture as seen in Fig. 4a. Since the input \mathbf{h}^{UL} is complex, we divide it into two feature channels (real and imaginary). More precisely, we use the complex DL channel estimate \mathbf{h}_i^{DL} and the predicted beam index \hat{y}_i to calculate the channel capacity in (2).

IV. EXPERIMENTS

A. Dataset generation

We use the publically available dataset generation framework DeepMIMO [8], which uses the Wireless InSite ray-tracing simulator [9] to generate the channels between the UEs and each base station. Specifically, we use the Outdoor 1 Blockage scenario where we utilize base stations on either side of the main street as clients in the FL terminology. For each UE position in the map, see Fig. 3, we generate an UL channel on a Sub-6GHz frequency band and a DL channel on a mmWave frequency band. Each UE position is in turn associated with the base station (client) for which the received DL signal is the strongest — this results in an unbalanced dataset. For each client, we set aside 20% of the client data as a test set for evaluation. For evaluation, we sample 5000 data samples with replacement from the test set in each run of the experiment.

In a decentralized setting it is common to have non-IID data that can be of non-identical client distributions [11], [16], [17]. In our case we generate data which can be characterized as having *quantity skew* (unbalancedness) and *concept shift* (same features, different label) [16].

B. Hyperparameters

Hyperparameters are tuned using Ray Tune [18] in four stages and used for all clients. For each model we tune the learning rate η , the number of hidden units in the fully connected layer, dropout, weight decay and learning rate decay rate. Additionally, for the IFCA case we tune J , λ [12], learning rate, ε -greediness [11] and server learning rate decay.

First, we tune the hyperparameters for a local model and for the case with two global cluster models $J = 2$. Thereafter, we tune the hyperparameters for the gating model using the best hyperparameters found in the earlier steps. Note that we use the *best* global cluster model and a local model as experts in the MoE. See Fig. 4b and [11] for details.

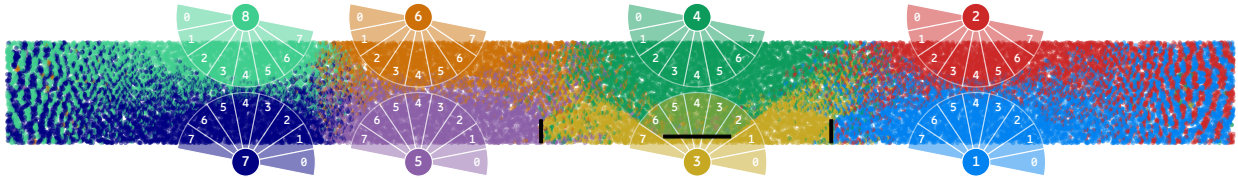
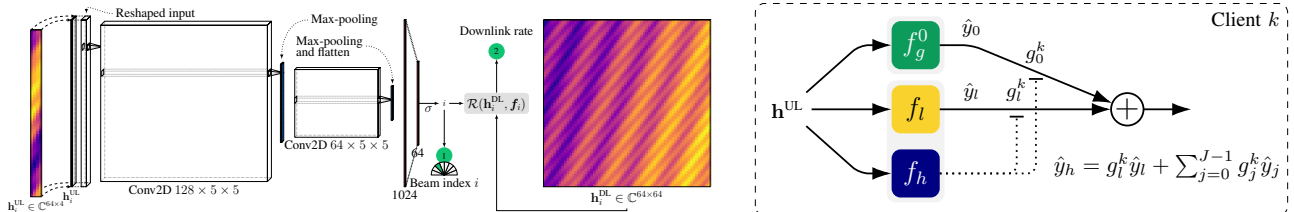


Fig. 3. **Dataset.** We use DeepMimo [8], [9] to generate the mmWave DL channels and Sub-6GHz UL channels for each of the 8 base stations. Each position is associated with the base station that has the strongest received signal in the DL. Note the order of the beam indices, here illustrated with 8 beams.



(a) **Neural Network architecture.** The complex UL channel estimate \mathbf{h}^{UL} is divided into two channels (real and imaginary) used as input to a CNN model. The DL channel estimate \mathbf{h}_i^{DL} is used to calculate the channel capacity.

(b) **Adaptive expert models.** Our approach adjusts to non-IID data distributions by adaptively training a Mixture of Experts (MoE) for clients that share similar data distributions.

Fig. 4. Combining CNN-models and a MoE is key to good performance when data shows non-IID characteristics.

Hyperparameters depend on the parameters of the data generation, but we tune the hyperparameters for the fixed case. The tuned hyperparameters are then used for all experiments.

C. Results

The optimal number of global cluster models. In Figs. 5a and 5b and Table I we explore the claim from [10] that IFCA is robust against setting the number of J cluster models to be larger than the anticipated clusters in the dataset. We set the fraction of training data samples per client to 10%. By utilizing the ε -greedy cluster assignment from [11] we avoid the mode-collapse problem of vanilla IFCA. We show that FEDAVG fails to outperform a local model, while FEDLION does, see Figs. 5a and 5b.

We note that for $J > 2$ we get approximately the same accuracy and channel capacity, see Fig. 5c, while the cost of storage and communication costs increases linearly. In Fig. 5d we see that the convergence is faster when clients are mapped to more suitable global cluster models. We set $J = 2$ for the remainder of the experiments. Note that the number of clients $K = 8$ is small and the fraction of participating clients C is 1.

The effect of increasing number of training data samples. In Fig. 6a we explore the effect of increasing the number of data samples on accuracy. We can easily see that our FEDLION approach is more sample efficient than the vanilla FEDAVG, i.e. the algorithm attains the same accuracy using fewer samples. For the same number of samples FEDLION, achieves a higher accuracy than FEDAVG. This result carries over to the top-3 accuracy seen in Fig. 6b and the effect is most prominent when we have few training data samples. Finally, we note that while FEDLION converges faster for a low fraction of training data used, FEDAVG converges faster when more than 10% of the training data is used per client, as shown in Fig. 6c.

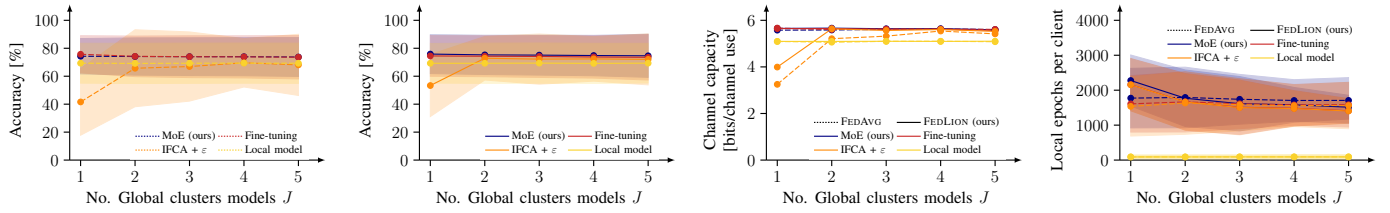
Varying ε -greediness. Our FEDLION outlined in Algorithm 1 method is more robust w.r.t. increasing ε , shown in Figs. 7a and 7d. The fraction of training data samples was 10%. We see in Fig. 7c that the convergence rate improves as ε increases. We hypothesise that this stems from the fact that the algorithm is robust against noisy updates due to its momentum term, and that this helps prevent overfitting. However, the effect on accuracy is not seen in the case of MoE, see Fig. 7b. FEDLION outperforms FEDLION for all values of ε .

Impact of Signal-to-noise ratio (SNR). To investigate the impact of Signal-to-noise ratio (SNR), we set the UL SNR for all data samples to be the same in one run of the experiment. The fraction of training data samples was 10%. In Fig. 8 we show the result on accuracy for IFCA with ε -greedy cluster assignment. Our FEDLION server-side optimization method achieves slightly higher accuracy than FEDAVG for IFCA, but the top-3 accuracy is indistinguishable between the two. For MoE the performance is similar for FEDLION and FEDAVG.

Training curves. Finally, we illustrate training curves for the first of the two global cluster models in Fig. 9. We see that initially, FEDAVG improves faster than FEDLION. However, FEDLION catches up and achieves higher performance.

V. RELATED WORK

ML-based beam alignment. The mmWave beam alignment problem has received great attention in recent years [19]–[21]. Most data-driven approaches in this area focused on supervised learning procedures to predict the best beam based on some form of feature side information [5]. For example, Echigo et al. [21] proposed a deep learning approach to predict an optimal narrow beam based on wide beams measurements, reducing the beam alignment overhead. Alrabeiah and Alkhateeb [5] used a neural network to predict the best beam in mmWave networks based on sub-6 GHz feature information. Our problem formulation was

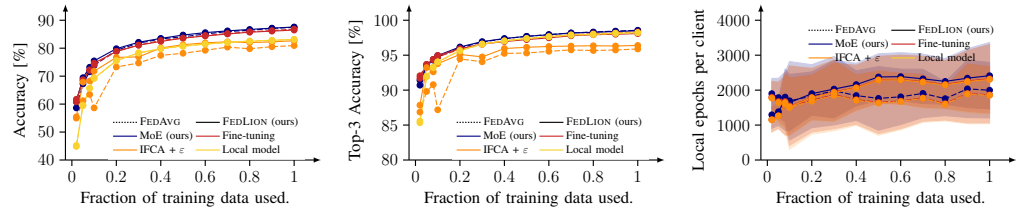


(a) Accuracy versus number of clusters for FEDAVG. (b) Accuracy versus number of clusters for FEDLION. (c) Channel capacity versus number of clusters for FEDAVG and FEDLION. (d) Complexity in terms of local epochs versus number of clusters.

Fig. 5. **The optimal number of global cluster models.** Performance of IFCA + ϵ , a model fine-tuned from the best global cluster model and our MoE when varying the number of clusters J for FEDAVG and FEDLION. The fraction of training data samples per client was 10%.

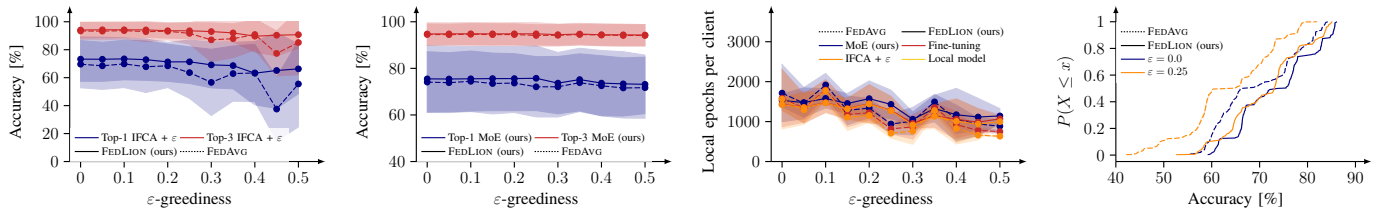
TABLE I
THE OPTIMAL NUMBER OF GLOBAL CLUSTER MODELS. ACCURACY VERSUS NUMBER OF CLUSTERS FOR FEDAVG AND FEDLION.

| Clusters | Method | # trials | MoE | | Local | | Fine-tuned | | IFCA + ϵ | |
|----------|----------------|----------|--------------|----------|-------|----------|------------|----------|-------------------|----------|
| | | | μ | σ | μ | σ | μ | σ | μ | σ |
| 1 | FEDAVG | 29 | 74.13 | 6.56 | 69.30 | 7.30 | 75.49 | 6.82 | 41.08 | 12.37 |
| | FEDLION (ours) | 43 | 75.87 | 7.12 | 69.28 | 7.27 | 74.52 | 7.40 | 53.33 | 11.49 |
| 2 | FEDAVG | 29 | 73.83 | 6.77 | 69.11 | 7.28 | 73.98 | 7.34 | 64.85 | 15.19 |
| | FEDLION (ours) | 42 | 75.28 | 7.22 | 69.25 | 7.31 | 74.25 | 7.50 | 72.89 | 7.94 |
| 3 | FEDAVG | 27 | 73.91 | 6.89 | 69.33 | 7.33 | 74.03 | 7.73 | 65.04 | 13.88 |
| | FEDLION (ours) | 42 | 75.12 | 7.24 | 69.39 | 7.34 | 74.17 | 7.60 | 71.96 | 9.40 |
| 4 | FEDAVG | 28 | 74.03 | 6.99 | 69.34 | 7.40 | 73.88 | 7.74 | 69.54 | 8.72 |
| | FEDLION (ours) | 41 | 74.76 | 7.40 | 69.21 | 7.30 | 73.73 | 7.72 | 72.48 | 8.17 |



(a) Accuracy versus fraction of training samples. (b) Top-3 accuracy versus fraction of training samples. (c) Complexity as local epochs versus fraction of training samples.

Fig. 6. **The effect of increasing number of training data samples.** Performance when varying the fraction of training samples for FEDAVG and FEDLION.



(a) Accuracy versus ϵ for IFCA. (b) Accuracy versus ϵ for MoE. (c) Complexity as local epochs vs. ϵ . (d) Accuracy ECDF.

Fig. 7. **Varying ϵ -greediness.** Performance when varying the ϵ -greediness in the IFCA cluster assignment for FEDAVG and FEDLION.

inspired by this work, but we devise a personalized FL approach to deal with the inherent non-IID nature of the mmWave channel. Tian et al. [19] studied a beam-alignment problem in mmWave vehicular network. They devise a personalized deep learning

approach which envision a pre-training phase on the complete dataset and a local fine-tuning phase on data from the specific base station. As opposed to our FL method, classical deep learning approaches require the training to be centralized; as a

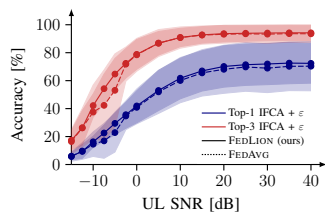


Fig. 8. **Impact of Signal-to-noise ratio (SNR)** for IFCA with ε -greedy cluster assignment.

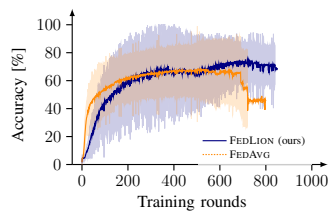


Fig. 9. **Training curves** for a IFCA global cluster model with ε -greedy cluster assignment.

consequence they are harder to scale and raise privacy concerns.

FL-based beam alignment. A few works investigated the beam alignment problem in FL [22], [23]. Elbir et al. [22] introduce an FL framework for hybrid beamforming using CNNs which predicts the best analog beamformers, based on channel data. Similarly, Chafaa et al. [23] employ an FL method to predict the optimal beamforming vector from a discrete beamforming codebook, based on Sub-6GHz channel data. Although these methods have the advantage of providing decentralized training and execution, and hence reducing communication overhead, they lack personalization and may lead to suboptimal beamforming configurations, especially in highly heterogeneous scenarios. To the best of our knowledge, this paper is the first to propose a personalized FL approach.

VI. DISCUSSION AND LIMITATIONS

There are many future directions of research stemming from this work. Firstly, and most importantly, these methods must be tested on a real-world dataset with more clients, where the environment is more complex and with a set of realistic beams. A real-world dataset will also have a *concept drift* non-IID characteristic (same labels, different features) [16] that we expect our MoE method to handle better than the concept shift characteristic. Secondly, the data volume is an important for the deployment of these methods in real mobile networks. Thirdly, the generalization aspect has not been investigated even though it is a major advantage of the MoE approach.

VII. CONCLUSIONS

In this paper we investigated the problem of selecting the best mmWave downlink beam in an analog beamforming scenario, when data has non-IID characteristics, specifically class imbalance, concept shift and unbalanced data — a more difficult problem than the problem solved in prior work.

We leveraged a personalized FL technique [11] that is able to adapt to non-IID characteristics and showed that it is robust to incorrectly setting the number of global cluster models.

In conclusion, we demonstrated higher sample-efficiency and higher accuracy than prior works by combining personalized FL with a server-side optimization method FEDLION. Furthermore, we provided insights and opportunities for future research and practical use of these methods.

ACKNOWLEDGMENT

We thank Y. Cheng for his inspirational Master’s thesis work and all reviewers for their critical feedback that enhanced the quality of this paper, especially Dr. A. Alam, Dr. A. Alabbasi, Dr. N. Jaldén, Dr. J. Jeong, D. Kolmas, Dr. I. Misioni, Dr. C. Svahn, G. Verardo, Assoc. Prof. Š. Girdzijauskas and Prof. S. Haridi.

This work was partially supported by the Wallenberg AI, Autonomous Systems and Software Program (WASP) funded by the Knut and Alice Wallenberg Foundation.

REFERENCES

- [1] “Leveraging the potential of 5G millimeter wave,” Ericsson AB, Tech. Rep., 2018. [Online]. Available: <https://www.ericsson.com/en/reports-and-papers/further-insights/leveraging-the-potential-of-5g-millimeter-wave>
- [2] M. Alrabeiah and A. Alkhateeb, “Deep Learning for TDD and FDD Massive MIMO: Mapping Channels in Space and Frequency,” in *IEEE 53rd Asilomar Conf. Sign., Syst., and Comput. (ACSSC), Pacific Grove, CA, USA*. IEEE, 2019, pp. 1465–1470. [Online]. Available: <https://doi.org/10.1109/IEEECONF44664.2019.9048929>
- [3] B. McMahan, E. Moore, D. Ramage, S. Hampson, and B. A. y Arcas, “Communication-Efficient Learning of Deep Networks from Decentralized Data,” in *Int. Conf. AI and Statistics (AISTATS), Fort Lauderdale, FL, USA*. PMLR, 2017. [Online]. Available: <http://proceedings.mlr.press/v54/mcmahan17a.html>
- [4] K. A. Bonawitz et al., “Towards Federated Learning at Scale: System Design,” in *Mach. Learn. and Syst. (MLSys), Stanford, CA, USA*, 2019. [Online]. Available: <https://doi.org/10.48550/arXiv.1902.01046>
- [5] M. Alrabeiah and A. Alkhateeb, “Deep Learning for mmWave Beam and Blockage Prediction Using Sub-6GHz Channels,” 2019. [Online]. Available: <https://doi.org/10.48550/arXiv.1910.02900>
- [6] I. Chafaa, R. Negrel, E. V. Belmega, and M. Debbah, “Federated Channel-Beam Mapping: from sub-6GHz to mmWave,” in *IEEE Wirel. Commun. and Netw. Conf. Workshop (WCNCW)*, Mar. 2021, pp. 1–6. [Online]. Available: <https://doi.org/10.1109/WCNCW49093.2021.9420006>
- [7] Y. Cheng, “Personalized Federated Learning for mmWave Beam Prediction Using Non-IID Sub-6 GHz Channels,” Master’s thesis, KTH Royal Institute of Technology, Jan. 2023.
- [8] A. Alkhateeb, “DeepMIMO: A Generic Deep Learning Dataset for Millimeter Wave and Massive MIMO Applications,” in *Inf. Theory and Appl. Workshop (ITA)*, San Diego, CA, Feb. 2019, pp. 1–8. [Online]. Available: <https://doi.org/10.48550/arXiv.1902.06435>
- [9] “Wireless InSite,” 2023. [Online]. Available: <https://www.remcom.com/wireless-insite-em-propagation-software>
- [10] A. Ghosh, J. Chung, D. Yin, and K. Ramchandran, “An Efficient Framework for Clustered Federated Learning,” in *Adv. Neural Inf. Process. Syst. (NeurIPS)*, 2020. [Online]. Available: <https://proceedings.neurips.cc/paper/2020/file/e32cc80bf07915058ce90722ee17bb71-Paper.pdf>
- [11] M. Isaksson, E. L. Zec, R. Cöster, D. Gillblad, and S. Girdzijauskas, “Adaptive Expert Models for Personalization in Federated Learning,” in *Trustworthy Federated Learning*. Springer, 2022, vol. 13448, pp. 1–16. [Online]. Available: https://doi.org/10.1007/978-3-031-28996-5_1
- [12] X. Chen et al., “Symbolic Discovery of Optimization Algorithms,” 2023. [Online]. Available: <https://doi.org/10.48550/arXiv.2302.06675>
- [13] K. Ma, Z. Wang, W. Tian, S. Chen, and L. Hanzo, “Deep Learning for mmWave Beam-Management: State-of-the-Art, Opportunities and Challenges,” *IEEE Wirel. Commun.*, pp. 1–8, 2022. [Online]. Available: <https://doi.org/10.1109/MWC.018.2100713>
- [14] P. Tillet, H. Kung, and D. D. Cox, “Triton: an intermediate language and compiler for tiled neural network computations,” in *ACM SIGPLAN Int. Workshop on Mach. Learn. and Program. Lang. (MAPL@PLDI), Phoenix, AZ, USA*, Jun. 2019, pp. 10–19. [Online]. Available: <https://doi.org/10.1145/3315508.3329973>
- [15] S. J. Reddi et al., “Adaptive Federated Optimization,” in *9th Int. Conf. Learning Representations (ICLR), Austria*. OpenReview.net, May 2021. [Online]. Available: <https://openreview.net/forum?id=LkFG31B13U5>
- [16] P. Kairouz et al., “Advances and Open Problems in Federated Learning,” *Found. Trends Mach. Learn.*, vol. 14, no. 1–2, pp. 1–210, 2021. [Online]. Available: <https://doi.org/10.1561/22000000083>

- [17] K. Hsieh, A. Phanishayee, O. Mutlu, and P. B. Gibbons, "The Non-IID Data Quagmire of Decentralized Machine Learning," in *Int. Conf. Mach. Learn. (ICML)*. PMLR, 2020. [Online]. Available: <http://proceedings.mlr.press/v119/hsieh20a.html>
- [18] R. Liaw, E. Liang, R. Nishihara, P. Moritz, J. E. Gonzalez, and I. Stoica, "Tune: A Research Platform for Distributed Model Selection and Training," 2018. [Online]. Available: <https://doi.org/10.48550/arXiv.1807.05118>
- [19] M. Tian, Z. Zhang, Q. Xu, and L. Yang, "A Personalized Solution for Deep Learning-Based mmWave Beam Selection," *IEEE Wirel. Commun. Lett.*, vol. 12, no. 1, pp. 183–186, 2023. [Online]. Available: <https://doi.org/10.1109/LWC.2022.3220956>
- [20] M. Tian, Z. Zhang, Q. Xu, and L. Yang, "A Privacy-Preserved Split Learning Solution for Deep Learning-Based mmWave Beam Selection," *IEEE Commun. Lett.*, vol. 26, no. 7, pp. 1474–1478, 2022. [Online]. Available: <https://doi.org/10.1109/LCOMM.2022.3170211>
- [21] H. Echigo, Y. Cao, M. Bouazizi, and T. Ohtsuki, "A Deep Learning-Based Low Overhead Beam Selection in mmWave Communications," *IEEE Trans. Veh. Technol.*, vol. 70, no. 1, pp. 682–691, 2021. [Online]. Available: <https://doi.org/10.1109/TVT.2021.3049380>
- [22] A. M. Elbir and S. Coleri, "Federated Learning for Hybrid Beamforming in mm-Wave Massive MIMO," *IEEE Commun. Lett.*, vol. 24, no. 12, pp. 2795–2799, 2020. [Online]. Available: <https://doi.org/10.1109/LCOMM.2020.3019312>
- [23] I. Chafaa, R. Negrel, E. V. Belmega, and M. Debbah, "Federated Channel-Beam Mapping: from sub-6GHz to mmWave," in *IEEE Wirel. Commun. and Netw. Conf. Workshop (WCNCW)*, Mar. 2021, pp. 1–6. [Online]. Available: <https://doi.org/10.1109/WCNCW49093.2021.9420006>

TABLE IV
TRAINING HYPERPARAMETERS RELATED FL AND FEDLION.

| Parameter | Value |
|----------------------------------|---------------------------|
| federated.lr | 0.003 416 91 |
| federated.server_lr | 0.000 272 589 |
| federated.lmbda | 0.000 463 701 |
| federated.fldropout | 0.583 516 |
| federated.fl_weight_decay | $2.102\ 18 \cdot 10^{-6}$ |
| federated.server_lr_decay_rate | $4.6406 \cdot 10^{-5}$ |
| federated.fl_local_lr_decay_rate | $1.008\ 85 \cdot 10^{-7}$ |
| federated.eps | 0.035 1229 |
| federated.flhiddenunits1 | 1024 |
| federated.flhiddenunits2 | 2048 |
| federated.epochs | 4000 |
| federated.fl_patience | 5 |
| federated.clusters | 2 |
| federated.frac | 1 |
| federated.local_bs | 256 |
| federated.local_ep | 3 |
| federated.flfilters1 | 128 |
| federated.flfilters2 | 64 |
| federated.filtersize | 5 |
| federated.server_optim | FedLion |
| federated.beta1 | 0.95 |
| federated.beta2 | 0.98 |
| federated.tau | 0.001 |

TABLE V
TRAINING HYPERPARAMETERS RELATED FL AND FEDAVG.

| Parameter | Value |
|----------------------------------|---------------------------|
| federated.lr | 0.017 951 6 |
| federated.server_lr | 0.001 323 05 |
| federated.fldropout | 0.728 812 |
| federated.fl_weight_decay | $1.342\ 72 \cdot 10^{-7}$ |
| federated.server_lr_decay_rate | 0.000 264 015 |
| federated.fl_local_lr_decay_rate | $5.8123 \cdot 10^{-7}$ |
| federated.eps | 0.005 020 87 |
| federated.lmbda | $3.116\ 22 \cdot 10^{-5}$ |
| federated.flhiddenunits1 | 1024 |
| federated.flhiddenunits2 | 2048 |
| federated.epochs | 4000 |
| federated.fl_patience | 5 |
| federated.clusters | 2 |
| federated.frac | 1 |
| federated.local_bs | 256 |
| federated.local_ep | 3 |
| federated.flfilters1 | 128 |
| federated.flfilters2 | 64 |
| federated.filtersize | 5 |
| federated.server_optim | FedAvg |
| federated.beta1 | 0.95 |
| federated.beta2 | 0.98 |
| federated.tau | 0.001 |

TABLE VI
TRAINING HYPERPARAMETERS RELATED TO FINE-TUNING OF FL MODELS.

| Parameter | Value |
|-----------------------------|--------------|
| finetuning.ft_lr | 0.000 117 23 |
| finetuning.ft_weight_decay | 0.262 46 |
| finetuning.ft_lr_decay_rate | 0.025 521 |
| finetuning.ft_patience | 10 |

TABLE VII
TRAINING HYPERPARAMETERS RELATED TO MOE MODELS AND FEDLION.

| Parameter | Value |
|-----------------------|---------------------------|
| moe.moe_lr | $5.129\ 69 \cdot 10^{-6}$ |
| moe.gate_dropout | 0.413 556 |
| moe.moe_lr_decay_rate | 0.000 790 47 |
| moe.gatefilters1 | 16 |
| moe.gatefilters2 | 0 |
| moe.gate_weight_decay | $2.157\ 71 \cdot 10^{-6}$ |
| moe.moe_epochs | 400 |
| moe.gatehiddenunits1 | 16 |
| moe.gatehiddenunits2 | 8 |
| moe.gatefiltersize | 5 |
| moe.moe_patience | 10 |

TABLE VIII
TRAINING HYPERPARAMETERS RELATED TO MOE MODELS AND FEDAVG.

| Parameter | Value |
|-----------------------|---------------------------|
| moe.moe_lr | $8.159\ 05 \cdot 10^{-6}$ |
| moe.gate_dropout | 0.554 633 |
| moe.gatehiddenunits1 | 4 |
| moe.moe_lr_decay_rate | 0.000 202 676 |
| moe.gatefilters1 | 16 |
| moe.gatefilters2 | 4 |
| moe.gate_weight_decay | $4.239\ 31 \cdot 10^{-6}$ |
| moe.moe_epochs | 400 |
| moe.gatehiddenunits2 | 8 |
| moe.gatefiltersize | 5 |
| moe.moe_patience | 10 |

TABLE IX
TRAINING HYPERPARAMETERS RELATED TO LOCAL MODELS.

| Parameter | Value |
|---------------------------|--------------|
| local.loc_epochs | 400 |
| local.local_lr | 0.001 097 89 |
| local.local_weight_decay | 0.023 695 5 |
| local.localdropout | 0.694 774 |
| local.local_lr_decay_rate | 0.021 437 9 |
| local.localhiddenunits1 | 1024 |
| local.localhiddenunits2 | 2048 |
| local.localfilters1 | 128 |
| local.localfilters2 | 64 |
| local.filtersize | 5 |
| local.local_patience | 10 |

TABLE II
DEEPMIMO [8] DATASET PARAMETERS.

| Parameter | DL | UL |
|------------------------------|------------------|------------------|
| scenario | 01_28B | 01_3p5B |
| num_paths | 5 | 15 |
| active_BS | [1, 2, ..., 8] | [1, 2, ..., 8] |
| user_row_first | 1 | 1 |
| user_row_last | 2200 | 2200 |
| row_subsampling | 1 | 1 |
| user_subsampling | 1 | 1 |
| enable_BS2BS | False | False |
| OFDM_channels | 1 | 1 |
| BS2BS_isnumpy | True | True |
| dynamic_settings.first_scene | 1 | 1 |
| dynamic_settings.last_scene | 1 | 1 |
| bs_antenna.shape | [1, 64, 1] | [1, 4, 1] |
| bs_antenna.spacing | 0.5 | 0.5 |
| bs_antenna.radiation_pattern | isotropic | isotropic |
| bs_antenna.rotation | None | None |
| ue_antenna.shape | [1, 1, 1] | [1, 1, 1] |
| ue_antenna.spacing | 0.5 | 0.5 |
| ue_antenna.radiation_pattern | isotropic | isotropic |
| OFDM.subcarriers | 512 | 32 |
| OFDM.subcarriers_limit | 64 | 64 |
| OFDM.subcarriers_sampling | 1 | 1 |
| OFDM.bandwidth | 0.5 GHz | 0.02 GHz |
| OFDM.RX_filter | 0 | 0 |
| scenario_params.carrier_freq | 28 GHz | 3.5 GHz |
| scenario_params.tx_power | 0 | 0 |
| scenario_params.num_BS | 12 | 12 |
| scenario_params.user_grids | [[1, 2751, 181]] | [[1, 2751, 181]] |

TABLE III
TRAINING HYPERPARAMETERS RELATED TO THE DATASET.

| Parameter | Value |
|-----------------------|-----------|
| data.n_data | -1 |
| data.n_data_test | 5000 |
| data.num_classes | 64 |
| data.channels | 2 |
| data.train_frac | 0.1 |
| data.eval_num_clients | 8 |
| data.num_clients | 8 |
| data.add_noise | physics |
| data.snr | 80 |
| data.ue_tx_power_dBm | 23 |
| data.bs_tx_power_dBm | 34 |
| data.noise_figure_dB | 5 |
| data.interference_dB | 0 |
| data.label_type | realistic |

APPENDIX

A. Hyperparameters

Hyperparameters used for the dataset generation are listed in Table II and for the training in Tables III to IX.

B. Acronyms

FEDADAGRAD Federated Adagrad 3
FEDADAM Federated Adam 3
FEDAVG Federated Averaging 1–7
FEDLION Federated EvoLved Sign Momentum 1, 3–7
FEDYOGI Federated Yogi 3
5G Fifth-generation technology standard 1, 2
AWGN Additive White Gaussian Noise 2
CNN Convolutional Neural Network 3–5
DL downlink, signal coming from a cell tower to your mobile device 1–4
FL Federated Learning 1–7
IFCA Iterative Federated Clustering Algorithm 1, 3–6
IID Independent and Identically Distributed 1–4, 6
Lion EvoLved Sign Momentum 1, 3
ML Machine Learning 2, 4
mmWave the band of spectrum with wavelengths between 10 millimeters (30 GHz) and 1 millimeter (300 GHz) 1–4, 6
MoE Mixture of Experts 1, 3–7
NR New Radio 2
SNR Signal-to-noise ratio 4
Sub-6GHz frequency bands under 6 GHz 1–4, 6
UE User Equipment 2, 3
UL uplink, signal leaving your mobile device and going back to a cell tower 1–4
ULA Uniform Linear Array 2
WASP Wallenberg AI, Autonomous Systems and Software Program 6

C. Symbols

B Subcarrier bandwidth 2
 β_1 Lion momentum hyper-parameter 3
 β_2 Lion momentum hyper-parameter 3
 C Fraction of clients selected 2–4
 Δ^k Client update 3
 Δ Client 3
 E local epochs 2
 ε ε -greedy parameter 3
 η Learning rate 3

\mathcal{F} Code book for downlink beamforming 2
 \mathbf{f} Generic code book, or downlink beamforming vector 2
 f_l Local model 4
 g_j^k Gate model weight for cluster model j and client k 4
 g_l^k Gate model weight for local model for client k 4
 \mathbf{h}_i^{DL} Downlink channel estimate 2–4
 \mathbf{h}_i^{DL} Downlink channel estimate sample i 2, 4
 \mathbf{h}_i^{UL} Uplink channel estimate 3, 4
 \mathbf{h}_i^{UL} Uplink channel estimate sample i 2–4
 i Data sample index 2, 3
 J Number of cluster models 3–5
 j Cluster model index 4
 K Number of clients 2–4
 k Client index 2–4
 K_s Number of selected clients 3
 L Number of subcarriers 2
 \mathcal{L} Estimated total loss 3
 l Beamforming vector index 2
 ℓ Loss function 3
 λ weight decay 3
 M Number of antennas 2
 m Momentum 3
 m Pre-coder weight index 2
 N Number of beams 2
 n Total number of data samples 2, 3
 n_k Number of data samples for client k 2, 3
 \mathcal{P} probability 3
 P_k Partition of dataset accessible to client k 2, 3
 $\{1, 2, \dots, K\}$ Population of clients 3
 s Subcarrier index 2
 S_t Selected set of clients at time t 2, 3
 t time in communication rounds 2, 3
 θ Beam angle 2
 \mathbf{w}_g Global model parameters 2, 3
 \mathbf{w}_k Local model parameters 3
 y Target of a data sample 3
 \hat{y}_h Estimated target (gating) 4
 \hat{y}_j Estimated target (cluster) 4
 \hat{y}_l Estimated target (local) 4
 y_i Ground truth class of data sample i 2, 3
 \hat{y}_i Predicted class of data sample i 2, 3